Axisymmetric Anisotropy I: Kinematics

Joe Dellinger and *Francis Muir*

INTRODUCTION

The assumption of isotropy pervades seismic data processing, and the presence of significant amounts of anisotropy can call into question the standard geophysical models. General anisotropy in three dimensions requires 21 elastic constants, and this seems beyond the resolving power of our geophysical tools. However, the inclusion of the axisymmetry constraint reduces the number of independent constants to 5, and would seem to provide a useful rock model, particularly in clastic basins, where azimuth-sensitive fracturing may be less of a factor than gravity-controlled laminar effects.

NORMAL MOVE OUT AND ANISOTROPY...

...Or, if anisotropy is such a big deal, why has NMO worked as the basis for time to depth conversions for 50 years?

Elliptic axisymmetric anisotropy adds the additional constraint that the impulse response have an elliptic cross section. This uses up one more elastic constant, leaving only 4 free. This special case is interesting because NMO appears to work perfectly with such a medium even when it doesn't. To see how this comes about, refer to figure 1. At the top a standard isotropic earth is depicted. The lines under the "X" represent "meter sticks", or some other arbitrary unit measure. In the diagram a point source has produced a circular wave front which will soon encounter the surface. Since the earth is isotropic, both the horizontal and vertical velocities are the same. The moveout is given by the standard (except for the factor of 2) NMO equation

$$t = \frac{1}{v}\sqrt{X^2 + Z^2}. \tag{1}$$

On the bottom we have the same diagram again, but stretched by a factor of σ horizontally, where $\sigma = v_x/v_z$ (about 1.4 for this figure). The formerly circular wavefront is now an ellipse. By stretching our model we have created an elliptically anisotropic earth. Equation 1 still applies, but our unit of measurement for X has been stretched. To convert back to our original

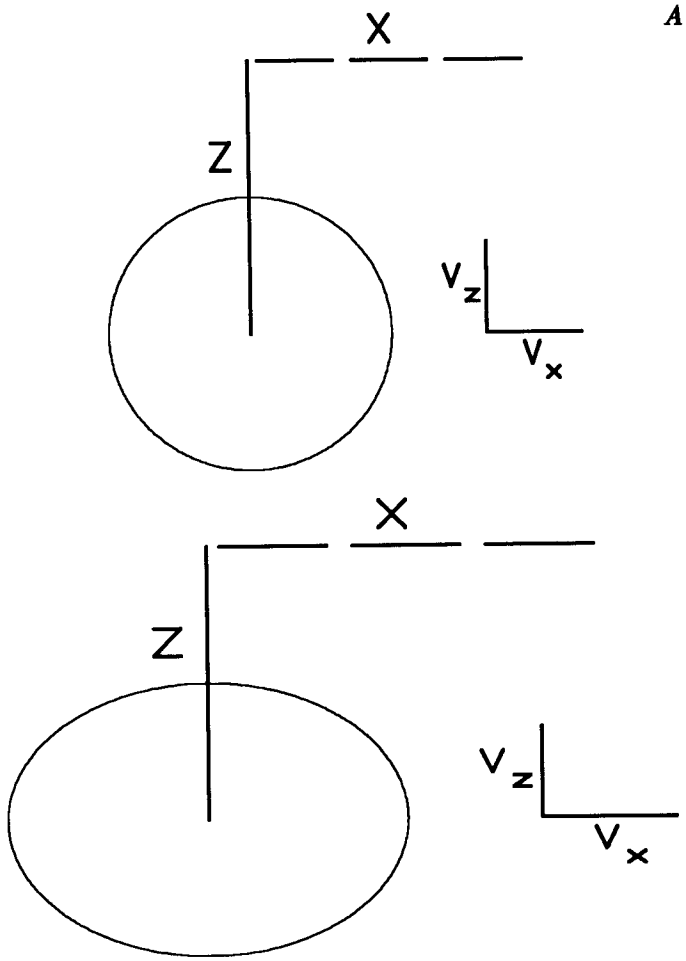

FIG. 1: Top: A representation of NMO in an isotropic earth. Bottom: A representation of NMO in an elliptically anisotropic earth.

units we must scale the X of equation 1 obtaining

$$t = \frac{1}{v_z}\sqrt{(\frac{X}{\sigma})^2 + Z^2}.$$

In NMO, v and Z are to be determined from the variation of t with X. Recasting our stretched equation in its original form, we get

$$t = \frac{1}{v_x}\sqrt{X^2 + (\frac{v_x}{v_z}Z)^2}. \tag{2}$$

Comparing equation 2 with equation 1, we see that NMO cannot distinguish an elliptically anisotropic earth from an isotropic one with an apparent velocity as the real horizontal one and with the apparent depth as the real depth multiplied by the ratio of the real horizontal to the real vertical velocity.

In general axisymmetric anisotropy the elliptic constraint will not be satisfied. However, for a broad range of angles an ellipse will usually fit the actual form of the wavefront quite accu-

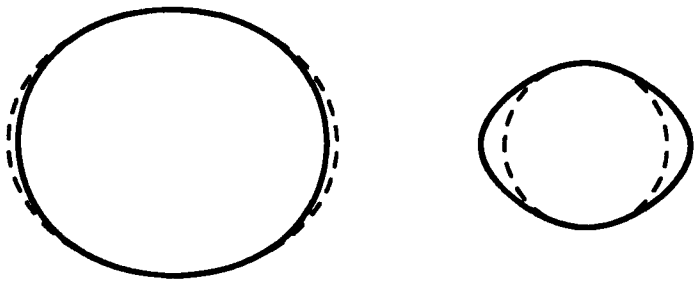

FIG. 2: Impulse responses with best-fitting ellipses for P waves for two shales. On the left is the "Cotton Valley shale", and on the right is the "Greenhorn shale".

rately. In this case it is the best-fitting ellipse for near-vertical propagation that will determine the NMO velocity.

In figure 2 are the computed impulse responses for P waves for two shales. The view shown is a "cross section". Since the shales were found to be transversely isotropic, any one cross section is the same as any other. This allows us to display the three-dimensional impulse response in only two dimensions. On the left is the computed impulse response for a shale from east Texas called the "Cotton Valley shale". Its elastic constants were measured by C. A. Tosaya (1982). On the right is the computed impulse response for a shale from the Greenhorn formation in the Williston basin which we will call the "Greenhorn shale". Its elastic constants were measured by Jones and Wang (1981). The two are shown to the same scale. The dotted line represents the best-fitting ellipse which determines the NMO velocity. Let us call the "apparent anisotropy" the ratio of the NMO velocity to the real vertical velocity. For the Cotton Valley shale this is 1.195 for P, .742 for S_v, and 1.162 for S_h. For the "Greenhorn shale" it is .948 for P, 1.882 for S_v, and 1.401 for S_h. Note that the apparent anisotropy for P waves tends to be smaller than that for S_v. If these two shales are typical, then it may very well be that even in the presence of strong anisotropy, P waves will often not *appear* anisotropic to NMO.

Before proceeding, it may be useful to refer to appendix 1 for a short review explaining notation. It may also be useful to refer to appendix 2 where the relationship between group velocity and phase slowness is discussed.

DIAGONALIZING THE WAVE EQUATION

The Christoffel equation is simply the wave equation Fourier transformed over every possible variable. The general 3-dimensional form of the equation is quite complicated. In the case of

axisymmetry about the z axis, however, it simplifies considerably to

$$\begin{bmatrix} C_{11}k_x^2 + C_{66}k_y^2 + C_{44}k_z^2 & (C_{12} + C_{66})k_xk_y & (C_{13} + C_{44})k_xk_z \\ (C_{12} + C_{66})k_xk_y & C_{66}k_x^2 + C_{11}k_y^2 + C_{44}k_z^2 & (C_{13} + C_{44})k_yk_z \\ (C_{13} + C_{44})k_xk_z & (C_{13} + C_{44})k_yk_z & C_{44}k_x^2 + C_{44}k_y^2 + C_{33}k_z^2 \end{bmatrix} \begin{bmatrix} v_x \\ v_y \\ v_z \end{bmatrix} = \rho\omega^2 \begin{bmatrix} v_x \\ v_y \\ v_z \end{bmatrix}.$$

Here C_{12} is not a free parameter, it is given by $C_{12} = C_{11} - 2C_{66}$. $\mathbf{v}$ is the particle velocity vector. The 3×3 matrix on the left side of the above equation is the Christoffel matrix. An eigenvector of this matrix gives the particle motion direction of a wave propagation mode, and the corresponding eigenvalue determines the velocity. The symmetry of this matrix implies that this equation has a complete set of orthogonal eigensolutions. This symmetry is a consequence of the symmetry of the stiffness matrix, which is required by energy conservation.

k_x, k_y, and k_z define a plane wave travelling in a particular direction. Axisymmetry implies that the x and y directions are equivalent. It is redundant to use both spatial coordinates. We will arbitrarily set $k_y = 0$, thus confining ourselves to the 2-dimensional cross section containing the x and z axes.

Since we are dealing with non-dispersive media, only the direction of the plane wave determines its velocity, not its wavelength. This can be incorporated into the notation by letting $k_x = k\sqrt{s}$ and $k_z = k\sqrt{1-s}$, where s is the *s*quare of the *s*ine of the angle between the direction of propagation of the plane wave and the symmetry axis (that is, $s = \sin^2\phi_w$), and $\frac{1}{k}$ is the wavelength of the plane wave.

Unfortunately, this change of variables loses the sign of k_x and k_z. However, examining the Christoffel equation we see that changing the sign of k_x merely changes the sign of v_x, and that changing the sign of k_z merely changes the sign of v_z. The zy and xy planes are mirror planes, and there is no loss of generality if we force k_x and k_z to both be positive.

Incorporating this change in notation, the Christoffel equation becomes

$$\begin{bmatrix} C_{11}s + C_{44}(1-s) & 0 & (C_{13} + C_{44})\sqrt{s(1-s)} \\ 0 & C_{66}s + C_{44}(1-s) & 0 \\ (C_{13} + C_{44})\sqrt{s(1-s)} & 0 & C_{44}s + C_{33}(1-s) \end{bmatrix} \begin{bmatrix} v_x \\ v_y \\ v_z \end{bmatrix} = \rho\left(\frac{\omega}{k}\right)^2 \begin{bmatrix} v_x \\ v_y \\ v_z \end{bmatrix}. \quad (3)$$

It is convenient to use prescience and make several convenient changes of variable at this point. We will let

$$\delta = C_{33} - C_{44},$$

$$\varepsilon = C_{11} - C_{44},$$

$$\eta = C_{66} - C_{44},$$

and

$$z = C_{13} + C_{44}.$$

We can also identify the term $\frac{\omega}{k}$ in equation 3 as the velocity V_w of the plane wave whose direction of propagation is determined by s. In terms of these new variables, the Christoffel equation becomes

$$\begin{bmatrix} \varepsilon s + \mathrm{C}_{44} & 0 & z\sqrt{s(1-s)} \\ 0 & \eta s + \mathrm{C}_{44} & 0 \\ z\sqrt{s(1-s)} & 0 & -\delta s + \mathrm{C}_{33} \end{bmatrix} \begin{bmatrix} v_x \\ v_y \\ v_z \end{bmatrix} = \rho {V_w}^2 \begin{bmatrix} v_x \\ v_y \\ v_z \end{bmatrix}. \tag{4}$$

One obvious solution of equation 4 is found by setting v_x and $v_z = 0$. Doing this, we obtain

$$\eta s + \mathrm{C}_{44} = \rho {V_w}^2 \quad \text{and} \quad \begin{bmatrix} v_x \\ v_y \\ v_z \end{bmatrix} = \mathrm{c} \begin{bmatrix} 0 \\ 1 \\ 0 \end{bmatrix}, \tag{5}$$

where c can be any arbitrary constant.

This is a *pure shear mode*, since the direction of propagation is always perpendicular to that of the particle motion. In standard terminology this propagation mode is called an $\mathrm{S_h}$ wave. Note that the phase slowness curve for this wave type is always elliptic. For reasons stated in appendix 2, this implies that the impulse response for this mode is also always elliptical. No matter how anisotropic the media may be, $\mathrm{S_h}$ waves will always have hyperbolic move out.

Since any two different eigensolutions are guaranteed orthogonal, the other 2 solutions of equation 4 must have $v_y = 0$. Substituting this in, we remove the solution we have already found and equation 4 reduces to

$$\begin{bmatrix} \varepsilon s + \mathrm{C}_{44} & z\sqrt{s(1-s)} \\ z\sqrt{s(1-s)} & -\delta s + \mathrm{C}_{33} \end{bmatrix} \begin{bmatrix} v_x \\ v_z \end{bmatrix} = \rho {V_w}^2 \begin{bmatrix} v_x \\ v_z \end{bmatrix}. \tag{6}$$

The solution of equation 6 is:

$$\tfrac{1}{2}\Big((\mathrm{C}_{33} + \mathrm{C}_{44}) + (\mathrm{C}_{11} - \mathrm{C}_{33})\mathrm{s} + \mathrm{m}\sqrt{(\mathrm{s}(\delta+\varepsilon) - \delta)^2 + 4\mathrm{s}(1-\mathrm{s})\mathrm{z}^2}\Big) = \rho {V_w}^2$$

and

$$\begin{bmatrix} v_x \\ v_y \\ v_z \end{bmatrix} = c \begin{bmatrix} 2z\sqrt{s(1-s)} \\ 0 \\ \mathrm{m}\sqrt{(s(\delta+\varepsilon) - \delta)^2 + 4s(1-s)z^2} - (\delta+\varepsilon)s + \delta \end{bmatrix}, \tag{7}$$

where m is either plus or minus one and c is once again an arbitrary constant.

The sign of m selects one of two propagation modes. Although not obvious from equation 7, the particle motion directions for these two propagation modes are always perpendicular. One important thing to notice is that the phase velocity for the $\mathrm{m} = 1$ solution is *always* greater than that for the $\mathrm{m} = -1$ solution for any s. Our isotropic intuition would suggest that the $\mathrm{m} = 1$ solution must be approximately a P wave and the $\mathrm{m} = -1$ solution approximately an $\mathrm{S_v}$ wave.

This is only true for materials reasonably close to being isotropic. To avoid bias, we will instead refer to the two solutions as the "fast" and the "slow" wave solutions.

Particle motion directions for these two wave types will be considered in detail in a following section. First, however, we shall find physical realizability constraints on the elastic constants.

ENERGY CONSTRAINTS

No energy should be produced by straining a material away from equilibrium. As shown in appendix 1, the strain energy density is given by

$$E = \frac{1}{2}\,\mathbf{S}^T \cdot \mathbf{C} \cdot \mathbf{S},$$

where $\mathbf{C}$ is the stiffness matrix. The requirement that the energy E be positive for any arbitrary non-zero strain $\mathbf{S}$ is exactly the requirement that the matrix $\mathbf{C}$ be positive definite. For an axisymmetric medium this matrix has the general form

$$\begin{bmatrix} C_{11} & C_{12} & C_{13} & 0 & 0 & 0 \\ C_{12} & C_{11} & C_{13} & 0 & 0 & 0 \\ C_{13} & C_{13} & C_{33} & 0 & 0 & 0 \\ 0 & 0 & 0 & C_{44} & 0 & 0 \\ 0 & 0 & 0 & 0 & C_{44} & 0 \\ 0 & 0 & 0 & 0 & 0 & C_{66} \end{bmatrix}, \tag{8}$$

where $C_{12} = C_{11} - 2C_{66}$.

Requiring the stiffness matrix as shown in equation 8 to be positive definite is equivalent to requiring that the following set of inequalities be satisfied:

$$C_{11} \geq C_{66} \geq 0, \quad C_{33} \geq 0, \quad C_{44} \geq 0, \quad \text{and} \quad C_{13}^2 \leq C_{33}(C_{11} - C_{66}). \tag{9}$$

In the isotropic case there are only two free elastic constants, C_{11} and C_{44}, and the isotropic energy constraints are:

$$\frac{3}{4}C_{11} \geq C_{44} \geq 0.$$

Since C_{11} and C_{44} determine the isotropic P and S wave velocities

$$V_p = \sqrt{\frac{C_{11}}{\rho}} \quad \text{and} \quad V_s = \sqrt{\frac{C_{44}}{\rho}},$$

in the this case P waves are always faster than S.

In the axisymmetric anisotropic case C_{44} (but not C_{66}) is allowed to be greater than C_{11} and C_{33}. As will be seen in the next section, as a consequence some kinds of S waves can actually have a higher velocity than P waves travelling in the same direction. This is an important difference from the isotropic case. Such a phenomenon cannot occur in that case because C_{44} and C_{66} are forced to be equal. The isotropic constraint on C_{44} is really one on C_{66} and C_{13}.

PARTICLE MOTION DIRECTIONS IN AXISYMMETRIC MEDIA

As we have already seen, one wave propagation mode is an S_h wave. Particle motion in this mode is perpendicular to both the z axis and to the direction of propagation. In the rest of this section we will be concerned with the other two solutions of the wave equation under axisymmetric anisotropy.

The particle motion directions are given by equation 7, but in an inconvenient form. It is better to write the formula in terms of the angle between the direction of plane wave propagation and the direction of particle motion. Let us call this angle ϕ_a, and let a be the square of the sine of this angle. Then (after a great deal of algebra):

$$a = \mathrm{m}\frac{\Big((2s-1)t_1 - t_2\Big)\sqrt{t_1^2 - t_2 z}}{2(t_2 z - t_1^2)} + \frac{1}{2},$$

where

$$t_1 = s(\delta + \varepsilon) - \delta \tag{10}$$

and

$$t_2 = 4s(s-1)z.$$

Note that since the eigensolutions are perpendicular, $a|_{\mathrm{m}=1} + a|_{\mathrm{m}=-1} = 1$.

Pure modes

Solving equation 10 to find when a is 0 or 1 yields conditions for the existence of pure P and S_v modes, respectively. The result is that pure P and S_v modes occur for 3 values of s:

$$s = 0, \qquad s = 1, \qquad \text{and} \qquad s = \frac{(\delta - z)}{(\delta - z) + (\varepsilon - z)}. \tag{11}$$

We shall consider the case $s = 0$ first. This corresponds to a plane wave travelling along the axis of symmetry. As shown by Auld (1973), waves travelling down a symmetry axis must always be pure modes. This is indeed the case we find here. There are two solutions, a pure P mode with velocity $\sqrt{\frac{C_{33}}{\rho}}$, and a pure S_v mode with velocity $\sqrt{\frac{C_{44}}{\rho}}$. There is an interesting complication here, though. The fast solution given when $\mathrm{m} = 1$ is the P one only if $\delta > 0$ (that is, if $C_{33} > C_{44}$). If $\delta < 0$, the fast solution is in fact the S_v one.

The case for $s = 1$ is very similar. Again we find that there are two pure modes, a P one with velocity $\sqrt{\frac{C_{11}}{\rho}}$, and an S_v one with velocity $\sqrt{\frac{C_{44}}{\rho}}$. The fast solution can again be either the P or S_v mode, whichever is faster.

The third pure mode direction given in equation 11 does not lie on any symmetry axis. It only exists if $\delta - z$ and $\varepsilon - z$ have the same sign. For this pure mode direction, if z is positive the fast solution is the P one and the slow solution is the S_v one. If z is negative, it is the other way around.

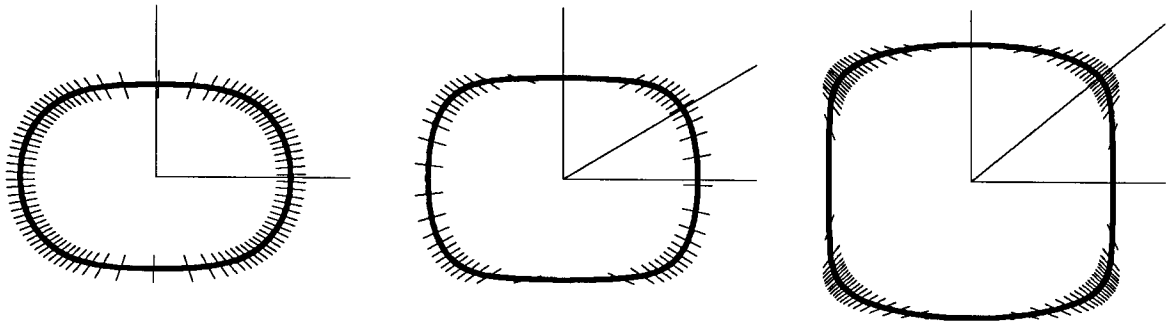

FIG. 3: The particle motion and impulse response of the fast solution for three different values of C_{44}, with C_{44} increasing to the right. The lines indicate the directions in which pure modes exist, and the "hairs" show the direction of particle motion.

Particle motion behavior

From what we have concluded so far it is clear that if any of δ, ε, or z is negative the particle motion must exhibit strange behavior. If exactly one of δ and ε is negative, for example, the same solution that is a P wave at $s = 0$ is an S_v wave at $s = 1$, and vice–versa. If δ and ε are of the same sign but z is not, then the solution that is a P wave at both $s = 0$ and $s = 1$ is a pure S_v wave somewhere in between! It is for such reasons that we cannot call the fast solution "Quasi-P" and the slow solution "Quasi-S_v", as is usually done in the literature.

Energy constraints do not permit δ, ε, and z to all be negative at the same time. This has the result that although the fast solution does not necessarily have to be close to a P wave for every angle, it does always have to be a pure P wave for *some* angle.

The three different sorts of particle motion behavior possible are shown in figure 3. All three are the impulse response for the fast solution, to the same scale. C_{44} is the only elastic constant that varies between them. z is positive for all three. None violate energy constraints. From left to right, the cases are: 1. both δ and ε positive, 2. δ negative and ε positive, and 3. both δ and ε negative. Also possible, but not shown, is the case where δ is positive and ε is negative. In this case the particle motion is approximately vertical all the way around. Allowing z to be negative does not add any new types of behavior.

Putting the sign back in the sine

Equation 10 is concise and in a convenient form, but is not useful computationally because it only gives the square of the sine of the angle of interest, ϕ_a. We will measure ϕ_a as positive in the same direction that ϕ_w is positive. As always, we assume that ϕ_w is between 0° and 90°.

Let s_3 be the third pure mode direction of equation 11. We will assume that z is positive, and refer to the angle for the fast solution. Then, if $\varepsilon > z$ and $\delta > z$, ϕ_a goes from negative to

positive as s goes from 0 to 1, with ϕ_a changing sign at $s = s_3$. If $\varepsilon < z$ and $\delta < z$, ϕ_a instead goes from positive to negative, again changing sign at $s = s_3$. If $\varepsilon > z$ and $\delta < z$, ϕ_a is always positive; if $\varepsilon < z$ and $\delta > z$, ϕ_a is always negative. If z is negative these same rules apply but we must reverse the given sign of ϕ_a and refer to the angle for the slow solution instead.

Very interesting, but is it real?

Some of the particle motion behaviors described here seem physically unlikely. However, some crystals are known to display quite perverse behavior. Auld, for example, examines one in his book (1973). Intuitively unlikely does not mean physically impossible.

BEHAVIOR OF THE IMPULSE RESPONSE AS A FUNCTION OF C_{13}

C_{13} has no part in determining either the vertical or horizontal velocity of either the fast or slow wave types. It controls the type of behavior in between, however, which is what makes it the most interesting elastic constant. (Note that C_{13} does not occur in any of the equations governing the S_h wave solution at all.)

Elliptic constraint

For the phase slowness and thus the impulse response to be an ellipse, ${V_w}^2$ must be a linear function of s. Recalling equation 7,

$$2\rho {V_w}^2 = (C_{33} + C_{44}) + (\varepsilon - \delta)s + m\sqrt{(s(\delta + \varepsilon) - \delta)^2 + 4s(1 - s)z^2}\,, \tag{12}$$

we see that this can only occur when the quantity under the radical is the square of a linear term that maintains the same sign over the interval 0 to 1. This occurs when either

$$z = \pm\sqrt{\delta\varepsilon} \quad (\text{if } \delta\varepsilon > 0) \qquad \text{or} \qquad z = 0 \quad (\text{if } \delta\varepsilon < 0). \tag{13}$$

If δ and ε are both negative, there are no solutions of equation 13 which are not prohibited by the energy constraints. This is easy to prove by showing that the minimal allowed value of z^2 is too large. However, if C_{66} is small, C_{11} and C_{33} are near in value, and C_{13} is as negative as allowed, ellipticity can still almost be reached.

If equation 13 is satisfied, both the fast and slow solutions will have an elliptical impulse response and dispersion relation. If δ and ε are both positive, the slow solution will in fact be circular. However, the particle motion will not be isotropic.

Types of behavior

The square root term causes deviation from an ellipse. It is this deviation which creates any interesting behavior of the phase slowness curve.

Under the square root is the sum of two terms, each of which is always positive. The second term is zero for $s = 0$ and $s = 1$ and maximal halfway in between. The first term is maximal at $s = 0$ and $s = 1$, and if δ and ϵ have the same sign, it passes through zero at

$$s_t = \frac{\delta}{\delta + \epsilon}. \tag{14}$$

The magnitude of z determines the relative weight of the two terms. If z is small, the first term dominates. This causes the phase slowness curve to bulge in for the slow solution and out for the fast solution at $s = s_t$. If δ and ϵ do not have the same sign, this term never passes through zero and so there is no resulting bulge. If z is large, the second term dominates. This causes the phase slowness to bulge in for the slow solution and out for the fast solution at $s = 0$ and $s = 1$.

This behavior is demonstrated in figure 4. The plot consists of two sections. The upper set of ten plots are dispersion relations; the lower set are their corresponding impulse responses. The light line is for the fast solution; the dark line is for the slow solution. All plots are to the same scale. z increases from left to right and top to bottom. Let us number them from 1 to 10 in this order.

Plot numbers 4, 6, and 9 have no special properties. They were inserted merely so that adjacent plots would not change too much. The rest of the plots, however, were chosen for their special properties. These are:

1. $z = 0$. In a sense this is the "minimal" value of z, because only z^2 occurs in the formulas. For this value the dispersion relation consists of two interlocking ellipses, with the slow solution traversing the outer parts and the fast solution the inner. Note that the vertical ellipse of the dispersion relation corresponds with the horizontal one of the impulse response, and vice–versa. In the direction s_t, the fast and slow solutions just touch. Unless C_{11} or C_{33} equal C_{44}, this is the only case in which the two solutions can do so.

2. Reality. These figures were calculated using the elastic constants of the "Greenhorn shale", but allowing C_{13} to vary. This figure is plotted using the real value of C_{13}. Note that the fast solution triplicates for this rock.

3. Here the dispersion relation of the slow solution is on the borderline between being concave and convex. As is shown in appendix 2, points of concavity of the dispersion relation are associated with points of triplications of the impulse response. "Borderline" triplications such as this one occur at angles where one of the two terms under the radical is zero. In this case it is the first term, and the triplication is at $s = s_t$.

5. For this plot the elliptic constraint is satisfied. Both the dispersion relation and impulse response are circular for the slow solution and elliptical for the fast.

7. and 8. Again we are at borderline triplications of the slow solution, at the top for 7 and

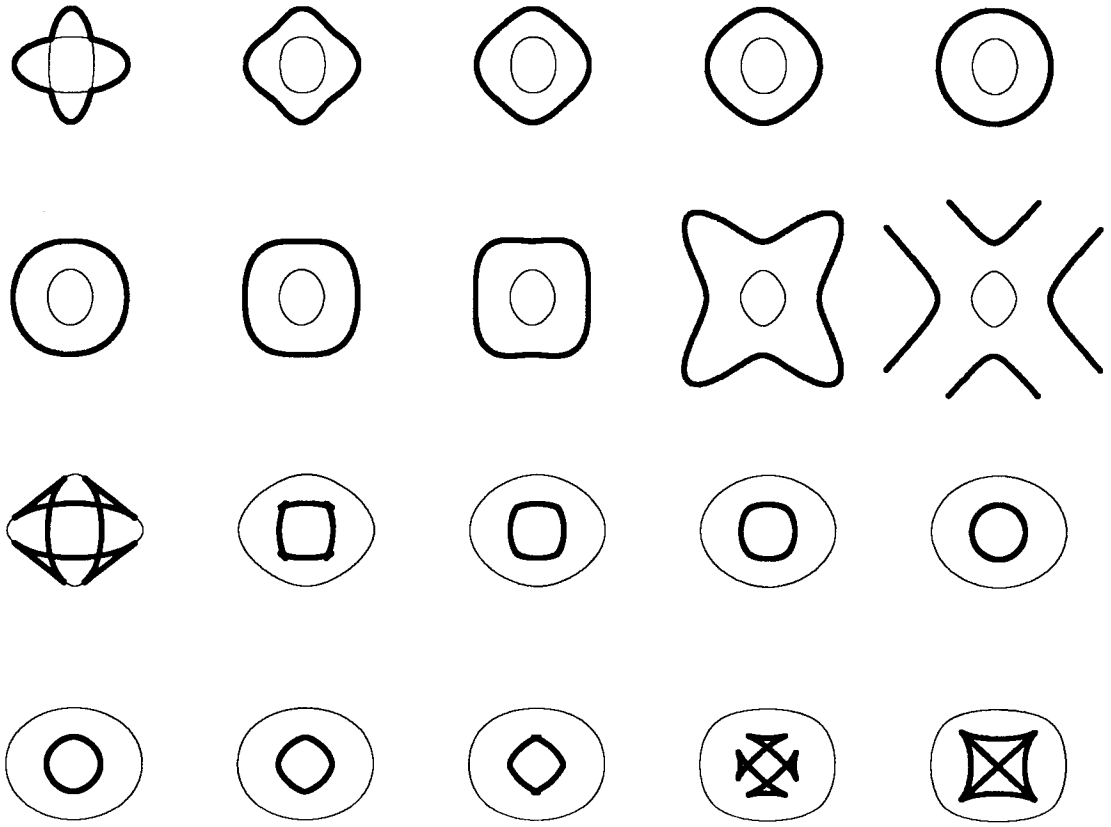

FIG. 4: Behavior of the dispersion relation (upper set) and impulse response (lower set) as a function of C_{13}. The dark line is the slow solution and the light line is the fast solution.

at the sides for 8. This time it is the second term which is zero at the triplications. Whether triplications first occur at the top or side depends on the relative sizes of C_{11} and C_{33}.

10. Both this and the previous plot violate the energy constraints. A weaker constraint is that the phase velocities must be positive for all s. This plot is just short of violating this constraint. This occurs when $C_{13} > \sqrt{C_{11}C_{33}}$.

Note that while the character of the slow solution changes dramatically, the fast solution changes only slowly, and with no major changes in behavior. If we had continued to increase z, the fast solution would have eventually also started to triplicate at $s = s_t$. However, this value of z is far outside the bounds of the energy constraint. This is in fact always the case, as will be shown in the next section.

If ϵ and δ are not of the same sign, the behavior is similar to that shown here but one of the two interlocking ellipses which occur in the first figure is missing, leaving a single ellipse. (This is the second solution to equation 13.)

Figure 5 shows how the transition from two ellipses to one occurs. z is zero in all the plots.

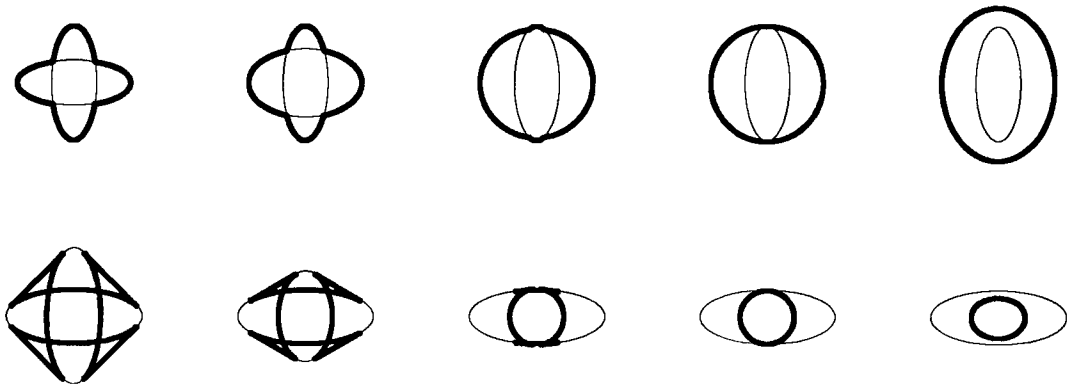

FIG. 5: Behavior of the dispersion relation (upper set) and impulse response (lower set) as a function of C_{33}. The dark line is the slow solution and the light line is the fast solution.

δ and ϵ start out positive and equal. δ is lowered in steps until it reaches zero in the second to last plot and finally becomes negative in the last. All plots are to the same scale. None violate energy constraints.

TRIPLICATIONS

It is difficult to migrate in the time domain if there are triplications, since energy can travel in the same direction with more than one velocity. Thus it is important to know for what ranges of elastic constants triplications do not occur.

From the previous section, we have a good idea as to the general shape of the dispersion relation as a function of z. We thus know to look for at most three different s for which borderline triplications can occur, and we know beforehand whether the values of z at each of these are upper or lower bounds. It is difficult, but straightforward, to derive analytical formulas that give the exact bounds. The results will be presented here.[1]

The top and side case

A borderline triplication occurs when $\frac{d\phi_r}{d\phi_w}$ and $\frac{d^2\phi_r}{d\phi_w^2}$ are simultaneously zero. For $s = 0$ and $s = 1$ the second derivative is always zero because of symmetry. Thus we need only solve for when the first derivative is zero. Using equation 28 at the end of appendix 2 this is not too difficult.

For $s = 0$, the result is that the fast solution can only triplicate if z^2 is negative – which means never. The slow solution triplicates when

$$z^2 > \begin{cases} +C_{11}\delta, & \text{if } \delta > 0; \\ -C_{44}\delta, & \text{if } \delta < 0. \end{cases} \tag{15}$$

[1]These formulas have all been verified empirically.

For $s = 1$ the result is the same, except that we must replace δ with ϵ and C_{11} with C_{33}.

The off–axis case

It is not obvious that the other triplication occurs at $s = s_t$. It is hopeless to evaluate $\frac{d^2\phi_r}{d\phi_w^2}$. The only way we were able to solve the problem was by guessing that $s = s_t$ might be the required angle and showing that this indeed was the case.

We started by rewriting equation 28 at the end of appendix 2 in the form of a formula whose sign indicates whether a triplication is occurring or not. This was evaluated at $s = s_t$, and after a great deal of algebra (being careful not to introduce unaccounted for spurious roots) was simplified to a third-degree polynomial in $|z|$. The derivative of the formula with respect to s was also computed and evaluated at $s = s_t$. This ultimately resulted after even more algebra in a fourth-degree polynomial, which was found to have as a factor the third-degree polynomial already derived. Thus as a function of s our original formula had only double roots at $s = s_t$, and so this was indeed the long sought after value of s at which borderline triplications occur.

Having thus proven our guess correct, the equation to solve is

$$|z|^3 + A|z| + B = 0,$$

where

$$A = -(3C_{44}^2 - C_{33}C_{44} - C_{11}C_{44} + 3C_{11}C_{33}) \tag{16}$$

and

$$B = -2\mathrm{m}|C_{11}C_{33} - C_{44}^2|\sqrt{\delta\epsilon}.$$

The solution to this polynomial is always of the form

$$|z| = 2\mathrm{m}\sqrt{-\tfrac{A}{3}}\cos\left(\tfrac{\phi+2\pi K}{3}\right),$$

where

$$\cos\phi = \sqrt{\tfrac{B^2}{4}/\tfrac{-A^3}{27}} \tag{17}$$

and

$$K = 0, 1, 2.$$

The $K = 0$ solution for $\mathrm{m} = -1$ and the $K = 1, 2$ solutions for $\mathrm{m} = 1$ are spurious, since $|z| \geq 0$ and these solutions are always negative. We know from the previous section that after the slow solution begins to triplicate at $s = s_t$, it continues to triplicate for higher values of $|z|$ until the energy constraints are violated. Thus the smaller of the two positive solutions of equation 17 for $\mathrm{m} = -1$ must be the solution we want. This is always the $K = 2$ solution. The $K = 1$ solution must therefore always violate the energy constraints. For $\mathrm{m} = 1$, only the $K = 0$ solution is not spurious. This solution is always larger than the $K = 1$ solution for $\mathrm{m} = -1$, and thus *the fast solution cannot triplicate in any direction for any physically allowed set of elastic constants.*

CONCLUSION

The fast solution is much more sensitive to the values of the elastic constants than the slow solution is. As a result the same energy constraints which merely keep the slow solution within the bounds of physical possibility constrain the behavior of the fast solution to a far greater extent. It may be for this reason that the assumption of isotropy has served geophysics so well for so long.

REFERENCES

Auld, B. A., 1973, Acoustic fields and waves in solids, vol. 1: John Wiley and Sons

Backus, G. E., 1962, Long-wave elastic anisotropy produced by horizontal layering: JGR, v. 67, p. 4427-4440

Claerbout, J. F., 1985, Imaging the earth's interior: Blackwell's Scientific Publications

Jones, E. A., and Wang, H. F., 1981, Ultrasonic velocities in Cretaceous shales from the Williston basin: Geophysics, v. 46, p. 288-297

Tosaya, C. A., 1982, Acoustical anisotropy of Cotton Valley shale: SPE technical paper 10995

APPENDIX 1

REVIEW OF THE CHRISTOFFEL EQUATION

Review of notation

The wave equation for a homogeneous medium is derived in a cartesian coordinate system by subdividing the medium into arbitrarily small cubes. The variables of interest are **u**, **S**, **T**, and **C**. [2]

u is called the particle displacement field. It gives the particle displacement as a function of position. It is not a good measure of strain because it is nonzero for both translations and rotations, neither of which deform the material at all and so should not be associated with strain. So instead of using **u** to measure strain the quantity

$$S_{ij}(\mathbf{r}) = \frac{1}{2}\left(\frac{\partial u_i}{\partial r_j} + \frac{\partial u_j}{\partial r_i}\right) \tag{18}$$

is used. The derivatives eliminate the effects of translations, while summing the two "symmetric" terms eliminates the effects of small rotations. Since we are only dealing with tiny deformations anyway, this is no restriction. S_{ij} is called the *strain matrix*. **u** is measured in distance units, whereas **S** is dimensionless. Note that **S** is always symmetric.

Now consider a unit cube. T_{ij} represents a force in the $+i$ direction on the area element facing the $+j$ direction. This is the *stress matrix*. It is measured in units of force per area. The anti-symmetric part of **T** is associated with torque. However, particle rotation plays no part in wave propagation. In the absence of external torque, the matrix **T** can thus be assumed symmetric.

The strain resulting from a given stress is a property of the medium involved. For small strains, the strain can be assumed to be a linear function of the stress. Since the strain matrix **S** and the stress matrix **T** are 3×3 matrices, they must be related by a 3×3×3×3 tensor. The elements of the tensor **C** are called *elastic stiffness constants*. Analytically,

$$T_{ij} = \mathrm{C}_{ijkl} S_{kl}. \tag{19}$$

C is measured in the same units as stress. The symmetries of **T** and **S** require that $\mathrm{C}_{ijkl} = \mathrm{C}_{jikl} = \mathrm{C}_{ijlk}$.

Abbreviated subscripts

Fourth order tensors are inconvenient to write down on paper. Usually **T**, **S**, and **C** are not

[2]Vector, matrix, and higher-order tensor quantities are identified by the use of **bold** type throughout this paper. For example, a 3-vector **X** has 3 scalar components: X_1, X_2, and X_3.

expressed with their natural subscripts but a compact notation is used instead. Symmetry allows each set of two subscripts to be replaced by one, with no attention to the order of the two subscripts: $xx \Longrightarrow 1$, $yy \Longrightarrow 2$, $zz \Longrightarrow 3$, $yz, zy \Longrightarrow 4$, $xz, zx \Longrightarrow 5$, and $xy, yx \Longrightarrow 6$. Thus an expression like C_{24} means C_{yyyz}, which we have already demonstrated is the same as C_{yyzy}. For some of the strain components there are multplicative factors of 2 as well. This transformation reduces $\mathbf{T}$ and $\mathbf{S}$ to 3-vectors, and $\mathbf{C}$ to a 6×6 matrix. The penalty for this conciseness is a loss of elegance and simplicity in the equations involved.

Strain energy

Assuming a perfectly elastic material, all of the energy put in while deforming it can be recovered by allowing the material to return to its equilibrium position. The energy expended in straining the material can be calculated in exactly the same way that the energy expended in stretching an ideal spring can. For a spring, the work expended is the integral of force over distance. For a general elastic material the corresponding quantity is the integral of the stress dotted with the differential strain. Mathematically, if $u_{\mathbf{S}_0}$ is the *strain energy density* associated with the strain $\mathbf{S}_0$, then

$$u_{\mathbf{S}_0} = \int_{\mathbf{0}}^{\mathbf{S}_0} d\mathbf{S}^T \cdot \mathbf{T}.$$

Using the relation $\mathbf{T} = \mathbf{C} \cdot \mathbf{S}$, this can be rewritten as

$$u_{\mathbf{S}_0} = \int_{\mathbf{0}}^{\mathbf{S}_0} d\mathbf{S}^T \cdot \mathbf{C} \cdot \mathbf{S}. \tag{20}$$

We will perform the integral in equation 20 along a path that goes directly from $\mathbf{0}$ to $\mathbf{A}$ and then directly from there to $\mathbf{S}_0 = \mathbf{A} + \mathbf{B}$. For the part from $\mathbf{0}$ to $\mathbf{A}$ we get:

$$\int_{\mathbf{0}}^{\mathbf{A}} d\mathbf{S}^T \cdot \mathbf{C} \cdot \mathbf{S} = \int_0^1 \mathbf{A}^T \cdot \mathbf{C} \cdot \mathbf{A}\, t\, dt = \frac{1}{2}\, \mathbf{A}^T \cdot \mathbf{C} \cdot \mathbf{A},$$

and for the part from $\mathbf{A}$ to $\mathbf{A} + \mathbf{B}$ we get:

$$\int_{\mathbf{A}}^{\mathbf{A}+\mathbf{B}} d\mathbf{S}^T \cdot \mathbf{C} \cdot \mathbf{S} = \int_0^1 \mathbf{B}^T \cdot \mathbf{C} \cdot (\mathbf{A} + \mathbf{B}t)\, dt = \frac{1}{2}\, \mathbf{B}^T \cdot \mathbf{C} \cdot \mathbf{B} + \mathbf{B}^T \cdot \mathbf{C} \cdot \mathbf{A},$$

for a combined integral over the entire path of

$$\frac{1}{2}\, (\mathbf{A}^T \cdot \mathbf{C} \cdot \mathbf{A} + \mathbf{B}^T \cdot \mathbf{C} \cdot \mathbf{B}) + \mathbf{B}^T \cdot \mathbf{C} \cdot \mathbf{A}. \tag{21}$$

Instead of the path chosen we might just as well have gone from $\mathbf{0}$ to $\mathbf{B}$ to $\mathbf{S}_0 = \mathbf{B} + \mathbf{A}$ instead. In that case we would have gotten

$$\frac{1}{2}\, (\mathbf{A}^T \cdot \mathbf{C} \cdot \mathbf{A} + \mathbf{B}^T \cdot \mathbf{C} \cdot \mathbf{B}) + \mathbf{A}^T \cdot \mathbf{C} \cdot \mathbf{B}. \tag{22}$$

The integral in equation 20 cannot depend on which of the two alternate paths we chose, for if it did we could go from the equilibrium position to $\mathbf{S}_0$ by one path and back again to equilibrium

by the other, and either create or destroy energy depending on which way we went! So the quantities in equations 21 and 22 must be equal for all $\mathbf{A}$ and $\mathbf{B}$. Since

$$\mathbf{A}^T \cdot \mathbf{C} \cdot \mathbf{B} = \mathbf{B}^T \cdot \mathbf{C}^T \cdot \mathbf{A},$$

this requires the existence of yet another symmetry property of the stiffness matrix, that

$$\mathbf{C} = \mathbf{C}^T.$$

Given this, the strain energy density associated with a particular strain $\mathbf{S}_0$ is

$$\frac{1}{2}\, \mathbf{S}_0^T \cdot \mathbf{C} \cdot \mathbf{S}_0,$$

regardless of how the material reached that strain state.

In the most general case, the stiffness matrix possesses no more symmetries than those already listed here. This leaves only $6+5+4+3+2+1 = 21$ independent elastic constants out of the original 81.

The Christoffel equation

The wave equation can be derived from three basic equations. These are the *strain-displacement relation*, relating $\mathbf{S}$ and $\mathbf{u}$, the *equation of motion*, relating $\mathbf{T}$ and $\mathbf{u}$, and the *elastic constitutive equation*, relating $\mathbf{T}$, $\mathbf{C}$, and $\mathbf{S}$. The first and third of these have already been given above in equations 18 and 19, respectively; the second is simply a restatement of Newton's law. Typically the three equations are solved for the particle velocity $\mathbf{v} = \frac{\partial \mathbf{u}}{\partial t}$.

If this is done, the result is of the form

$$\mathbf{M} \cdot \mathbf{C} \cdot \mathbf{M}^T \cdot \mathbf{v} = \rho \frac{\partial^2}{\partial t^2} \mathbf{v},$$

where $\mathbf{M}$ is a matrix of partial derivatives over the spatial coordinates. This can be fourier transformed over all three spatial variables and time, resulting in a purely algebraic equation of the same form. This is called the *Christoffel equation*, and the matrix $\mathbf{M} \cdot \mathbf{C} \cdot \mathbf{M}^T$ is called the *Christoffel matrix*. The eigenvalues of the Christoffel matrix are velocities, and the eigenvectors are particle motion directions.

If a medium is symmetric under certain transformations of coordinates, then any mathematical equation representing some property of the medium must also have corresponding symmetries. Thus, for a given crystal symmetry group the stiffness matrix $\mathbf{C}$ (and thus the Christoffel equation) can be simplified to take advantage of the symmetries that are present. The more symmetries there are, the simpler the Christoffel equation for the medium becomes. Christoffel equations for each symmetry group are given in appendix 3A of Auld's book Acoustic Fields and Waves in Solids, Volume I (1973). It can be shown by examining the stiffness matrix that as far as elastic properties are concerned axisymmetry is equivalent to the hexagonal symmetry system.

APPENDIX 2

FROM THE DISPERSION RELATION TO THE IMPULSE RESPONSE, AND BACK AGAIN

Group and phase velocity

The *phase velocity* associated with a given direction is the velocity of a plane wave travelling in that direction. The *group velocity* associated with a given direction is the velocity of a blob of energy travelling in that direction. Phase velocities are easier to calculate and more tractable mathematically, but since infinite uniform plane waves are hard to come by in the real world the group velocity is the more important quantity.

In axisymmetric anisotropy we need only specify the angle between the direction of propagation and the axis of symmetry. This allows us to treat the problem as a 2-dimensional one. We will label the group velocity V_r (r for $r$ay). It is a function of the group propagation angle, ϕ_r. Similarly, we will let V_w (w for $w$ave) be the phase velocity, and it will be a function of the plane wave propagation angle, ϕ_w.

The polar graph of V_w versus ϕ_w, the *group velocity curve*, is easy to picture physically. It is a snapshot of the wavefront created by the explosion of an ideal point source. Mathematically, it is the outer discontinuity of the point Green's function of the wave equation which describes propagation in the medium. The point Green's function is also known as the *impulse response* of the equation. It is important because any arbitrary source function can be easily decomposed into a sum of weighted impulses. Since the wave equation is linear the sum of the weighted impulse responses gives the wavefield produced by the original arbitrary source function.

A point source is mathematically equivalent to a source of plane waves which radiates equally in all directions. On a small enough scale any piece of a wavefront (except at a caustic) is indistinguishable from a plane wave. Since the group velocity curve represents the wavefront created by a point source, the tangent line to the group velocity curve at any point represents a single plane wave component radiated by the point source. We can find the velocity of such a plane wave component by measuring the distance it has travelled from the point source. The direction of travel of any plane wave is always given by the wavefront normal. (Uniform plane waves can't slip "sideways" as they travel, because motion in that direction makes no difference and is ignored.) Thus, for each V_r and ϕ_r we can construct a corresponding V_w and ϕ_w. Mathematically this entire process is merely integrating the point Green's function to obtain a line Green's function. Only bothering to look at the tangent line is the same approximation as is made when evaluating integrals by the method of stationary phase.

The process is shown geometrically in figure 6. The light solid curve represents the group

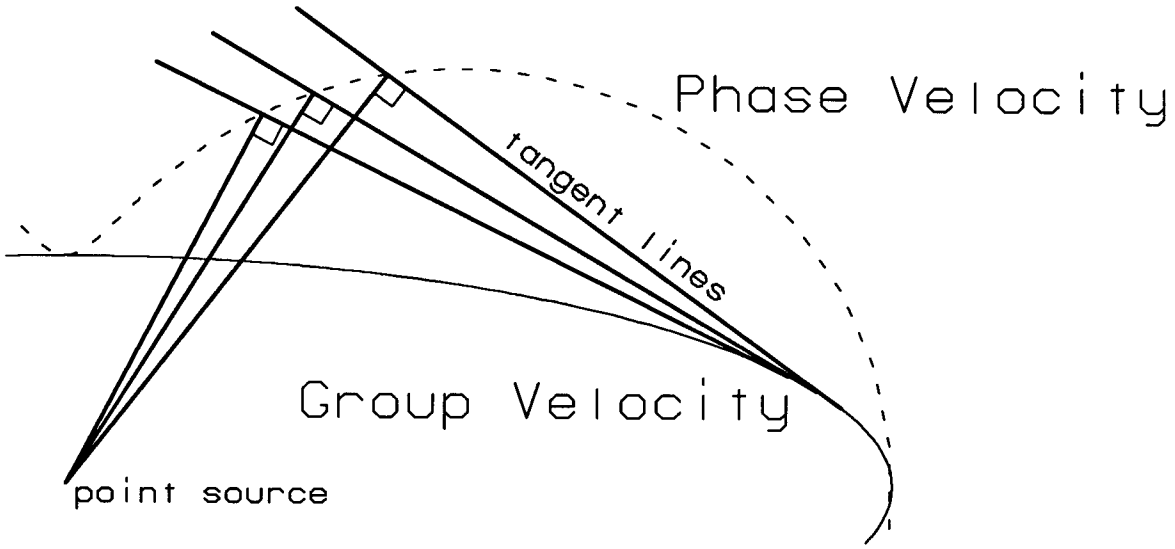

FIG. 6: A diagram showing the geometrical relationship between the group velocity curve (solid) and the phase velocity curve (dotted). In this example the group velocity curve is an ellipse.

velocity, and the light dotted curve the phase velocity. For each of three points on the group velocity curve, a dark tangent line has been drawn. A second dark line has been drawn from the point source to each tangent line so as to meet it at a right angle. The direction of the second line gives the direction of propagation of the plane wave represented by the tangent. Since the point of intersection of the two lines is also the point on the tangent line that is closest to the point source, the length of the second line is proportional to the phase velocity of the plane wave. Thus the locus of such intersections sweeps out the phase velocity curve.

Why should we care about the phase velocity?

The aim of this paper is to characterize the behavior of the impulse response of an axisymmetric anisotropic medium given only the 5 elastic constants. It is easy to solve the wave equation in terms of plane wave solutions; that is what Fourier transforming is all about. Instead of a complex differential equation we have a simple algebraic one. The drawback is that we do not get impulse responses for our solutions but instead plane wave velocities, which is to say a phase velocity curve.

Phase velocity curves are not much used in geophysics, but a closely related quantity is — the *dispersion relation*. A dispersion relation is simply the Fourier transform of a scalar wave equation. It has the form of an algebraic formula relating ω, k_x, and k_z. For a vector wave equation, there will be a different dispersion relation for each distinct mode of wave propagation.

Dispersion relations are useful because such a formula can be solved for k_z and used to downward and upward continue wavefields.

When graphed, the dispersion relation is a plot of $\frac{k_z}{\omega}$ versus $\frac{k_x}{\omega}$ for ω fixed. The spatial frequency k of a wave is $\sqrt{k_x^2 + k_y^2}$, and the tangent of the direction of propagation is $\frac{k_x}{k_z}$, so in polar coordinates the dispersion relation is a graph of $\frac{k}{\omega}$ as a function of direction. From basic Fourier transform theory, $V_w = \frac{\omega}{k}$. Let us call the inverse of velocity *slowness*, and let us represent it by an upside-down V: $A_w = \frac{k}{\omega}$. Thus a graph of a dispersion relation is also a graph of *phase slowness* for a particular temporal frequency. If a wave equation is *dispersive*, then the phase velocity is a function of frequency. The wave equations we examine in this paper are not dispersive, and so our graphs do not depend on frequency.

The most important property of the phase velocity, though, is that it is single valued. The essence of a linear wave equation is that it support solutions in the form of travelling sine waves. The velocity of such a wave may depend upon its direction of motion and spatial frequency. However, given a direction and a frequency, there should be only one velocity (possibly complex). A sine wave cannot travel with more than one velocity and stay the same.

Now for the math...

It is a simple exercise in trigonometry to find a mathematical formula for V_w and ϕ_w in terms of V_r and ϕ_r using the construction shown in figure 6. The result is:

$$V_w = \frac{{V_r}^2}{\sqrt{{V_r}^2 + (\frac{dV_r}{d\phi_r})^2}} \quad \text{and} \quad \phi_w = \phi_r - \text{Arctan}(\frac{dV_r/d\phi_r}{V_r}). \tag{23}$$

Equation 23 is not very useful. We usually need to go in the other direction, from the dispersion relation to the phase velocity to the group velocity. It is not obvious how to invert equation 23, though. It is most easily done by returning to the physical analogy used to derive equation 23.

The phase velocity curve gives the velocities of plane waves as a function of their direction of travel. Let us examine a pair of plane waves travelling in very nearly the same direction. The plane waves, being infinite non-parallel lines, must cross somewhere. The point where the waves cross is the point of highest amplitude. If more waves are used, instead of a point there will be a region in which the waves add constructively. Outside of this region the waves will add in a more or less random manner and mostly cancel. Summing a group of plane waves travelling in a narrow range of directions thus results in a moving blob of energy. The velocity of this blob is the group velocity.

We can now return to figure 6 and examine it in the terms of the preceding paragraph. In the figure we are summing three plane waves, using the phase velocity curve to position each

one at the correct distance from the source. The curve along which they are summing constructively must be tangent to each plane wave and also pass through the region where they intersect. The group velocity curve shown satisfies these requirements. In the limit as infinitely close plane waves are used, each point on the phase velocity curve can be identified with a unique point on the group velocity curve. As before, the position of this point gives V_r and ϕ_r.

It is an elementary exercise in calculus and trigonometry to find V_r and ϕ_r in terms of V_w and ϕ_w using this construction. The result is:

$$V_r = \sqrt{{V_w}^2 + (\frac{dV_w}{d\phi_w})^2} \quad \text{and} \quad \phi_r = \phi_w + \text{Arctan}(\frac{dV_w/d\phi_w}{V_w}). \tag{24}$$

This equation is useful, because in this paper V_w is a predetermined single-valued function of ϕ_w. The aim of the paper is to discover the properties of V_r. Since V_r is not a single-valued function of ϕ_r, it is most convenient to leave it in terms of ϕ_w.

We now have all the mathematics required to go from the dispersion relation to the impulse response. There are a few more properties of the phase and group velocities worth pointing out here, however.

Interesting symmetries

Earlier we introduced the concept of slowness. What do equations 23 and 24 look like in terms of slownesses? Equation 23 becomes:

$$\Lambda_w = \sqrt{\Lambda_r^2 + (\frac{d\Lambda_r}{d\phi_r})^2} \quad \text{and} \quad \phi_w = \phi_r + \text{Arctan}(\frac{d\Lambda_r/d\phi_r}{\Lambda_r}), \tag{25}$$

and equation 24 becomes:

$$\Lambda_r = \frac{\Lambda_w^2}{\sqrt{\Lambda_w^2 + (\frac{d\Lambda_w}{d\phi_w})^2}} \quad \text{and} \quad \phi_r = \phi_w - \text{Arctan}(\frac{d\Lambda_w/d\phi_w}{\Lambda_w}). \tag{26}$$

The symmetry between equations 23 and 26 and 24 and 25 is rather obvious. Our geometrical construction with which we connected the group and phase velocity curves also connects the phase and group slowness curves! From this construction, we can see that the phase velocity direction is perpendicular to the group velocity curve. By symmetry, the group slowness direction must also then be perpendicular to the phase slowness curve. An important consequence of this is that the group slowness (and also the group velocity) is a single-valued function of ϕ_r if and only if the phase slowness curve is convex.

Some of these relations are also derived in a different way in section 4.2 of Jon Claerbout's book Imaging the Earth's Interior. This book was also released as SEP–40.

Magic properties of ellipses

In an isotropic medium, the group and phase velocity curves are both circles. Since one over a constant is still a constant, the group and phase slowness curves are also circular. If we stretch a coordinate axis, our isotropic medium becomes elliptically anisotropic, and our circular group velocity curve becomes an ellipse. The similarity theorem of Fourier transforms tells us that if we stretch the x axis, say, then in the Fourier domain we have squeezed the k_x axis. This shows that our formerly circular dispersion relation in this case also becomes an ellipse. Thus, an elliptical group velocity goes with an elliptical phase slowness and vice-versa. While this property is easy to prove in this way, there seems to be no obvious proof using the geometric sort of methods that served so well earlier in this appendix (hence the term "magic"). An "inverse" ellipse is rather strange looking, as one can see by looking at the phase velocity curve in figure 6.

Triplications

Under what conditions can V_r become a multi-valued function of ϕ_r? As ϕ_w increases, ϕ_r generally also increases. As ϕ_w goes around the circle once, so does ϕ_r, and in fact they can never get more than 90° apart. If this general trend is always the case, then V_r is a single-valued function of ϕ_r as well as ϕ_w, and the impulse response is well behaved. Trouble occurs when ϕ_r instead of continuing forward stops and goes backwards for a while. When this happens, the same value of ϕ_r is assumed for three different values of ϕ_w. For this reason, such an event is termed a *triplication*.

A triplication thus occurs whenever

$$\frac{d\phi_r}{d\phi_w} < 0. \tag{27}$$

The formula for $\frac{d\phi_r}{d\phi_w}$ is a bit too messy to give here since it is easy to derive. Here we are only concerned with finding an inequality equivalent to that in equation 27. Multiplying through by a factor that is guaranteed to be always positive followed by a bit of algebra reduces the above inequality to:

$$\frac{d^2 V_w}{d\phi_w^2} < -V_w. \tag{28}$$

Although equation 28 seems innocent enough, the algebra it entails can be so horrendous that I do not recommend that anyone attempt to tackle this problem without a good symbolic algebra program at their side.[3]

[3]For this purpose we used MACSYMA, a large symbolic manipulation program developed at the MIT Laboratory for Computer Science, and currently available through Symbolics, Inc.

c13=107.00 zet=161.00
c11=341.00 c33=227.00 eps=287.00
c44=54.00 c66=106.00 del=173.00

Greenhorn shale